Gate capacitance coupling of singled-walled carbon nanotube thin-film transistors

Qing Cao, Minggang Xia,[a] Coskun Kocabas, Moonsub Shim, and John A. Rogers[b),c)]
Department of Chemistry, Department of Materials Science and Engineering, and Department of Physics, University of Illinois at Urbana-Champaign, Urbana, Illinois 61801

Slava V. Rotkin[b),d)]
Department of Physics, Lehigh University, Bethlehem, Pennsylvania 18015 and Center for Advanced Materials and Nanotechnology, Lehigh University, Bethlehem, Pennsylvania 18015

(Received 30 September 2006; accepted 11 December 2006; published online 12 January 2007)

The electrostatic coupling between singled-walled carbon nanotube (SWCNT) networks/arrays and planar gate electrodes in thin-film transistors (TFTs) is analyzed both in the quantum limit with an analytical model and in the classical limit with finite-element modeling. The computed capacitance depends on both the thickness of the gate dielectric and the average spacing between the tubes, with some dependence on the distribution of these spacings. Experiments on transistors that use submonolayer, random networks of SWCNTs verify certain aspects of these calculations. The results are important for the development of networks or arrays of nanotubes as active layers in TFTs and other electronic devices. © *2007 American Institute of Physics*. [DOI: 10.1063/1.2431465]

Single-walled carbon nanotube (SWCNT) networks/ arrays show great promise as active layers in thin-film transistors (TFTs).[1] Considerable progress has been made in the last couple of years to improve their performance and to integrate them with various substrates, including flexible plastics.[2,3] Nevertheless, the understanding of the physics of the electrostatic coupling between SWCNT networks/arrays and the planar gate electrode, which is critical to device operation and can be much different than that in conventional TFTs, is not well established. The simplest procedure, which has been used in many reports of SWCNT TFTs, is to treat the coupling as that of a parallel plate capacitor, for which the gate capacitance C_i is given by $\varepsilon/4\pi d$, where ε and d are the dielectric constant and the thickness of gate dielectric, respectively. This procedure enables a useful approximate evaluation of device level performance,[4–6] but it is quantitatively incorrect especially when the average spacing between SWCNTs is large compared to the thickness of the dielectric.[7] Since C_i critically determines many aspects of device operation, accurate knowledge of this parameter is important both for device optimizing, device designs, and for understanding basic transport mechanisms in the SWCNT networks/arrays.

In this letter, we use a model system, illustrated in Fig. 1, consisting of a parallel array of evenly spaced SWCNTs fully embedded in a gate dielectric with a planar gate electrode to examine capacitive coupling in SWCNT TFTs. The influence of nonuniform intertube spacings is also evaluated to show the applicability of those results to real devices. Results obtained in the single subband quantum limit and those obtained in the classical limit agree qualitatively in the range of dielectric thicknesses and tube densities (as measured in number of tubes per unit length) explored here. The models are used to analyze experiments on SWCNT network TFTs. These results provide insights into factors that limit the effective mobilities (μ) achievable in these devices.

We begin by calculating C_i of the model system in the quantum limit, where the charge density of the SWCNT in the ground state has full circular symmetry.[8] In this case, the charge distributes itself uniformly around the tube, and each tube, when tuned to the metallic region, can be treated as a perfectly conducting wire with radius R and uniform linear charge density ρ. The electrostatic potential induced by such a perfect conducting wire is $\phi(r)=2\rho\log(R/r)$, where r is the distance away from the center of the wire. The potential generated by an array of such wires is also a linear function of ρ and, in general, the induced potential at the ith tube depends on ρ of every tube in array according to

$$\phi_i^{\text{ind}}([\rho_j]) = \sum_j C_{ij}^{-1}\rho_j, \tag{1}$$

where coefficients of inductive coupling between ith and jth tube C_{ij}^{-1} are geometry dependent.[9]

For SWCNTs in the metallic regime, ρ is proportional to the shift of the Fermi level which is itself proportional to an average acting potential at the nanotube according to

$$\rho = -C_Q\phi^{\text{act}} = -C_Q(\phi^{\text{xt}} + \phi^{\text{ind}}), \tag{2}$$

where the proportionality coefficient is the quantum capacitance C_Q.[8,10,11] This equation is written to separate contributions from the external potential ϕ^{xt} as applied by distant electrodes and as generated by any other external source associated with charge traps, interface states, etc., and the induced potential ϕ^{ind} as given by Eq. (1).

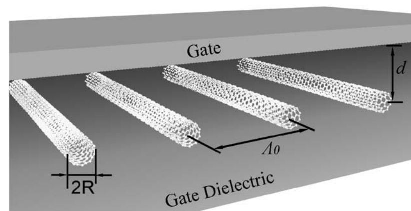

FIG. 1. Schematic illustration of the model system. R is the nanotube radius; the distance between each tube and the dielectric thickness are Λ_0 and d, respectively.

[a]Present address: Department of Physics, Xian Jiaotong University, Xian, China.
[b]Author to whom correspondence should be addressed.
[c]Electronic mail: jrogers@uiuc.edu
[d]Electronic mail: rotkin@lehigh.edu

0003-6951/2007/90(2)/023516/3/$23.00 © 2007 American Institute of Physics
Downloaded 12 Jan 2007 to 130.126.101.208. Redistribution subject to AIP license or copyright, see http://apl.aip.org/apl/copyright.jsp

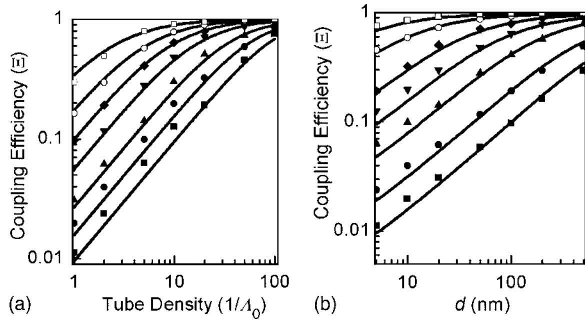

FIG. 2. (a) Capacitance ratio (Ξ) calculated by FEM vs linear SWCNT densities ($1/\Lambda_0$) for d ranging from 5 nm (□), 10 nm (●), 20 nm (▲), 50 nm (▼), 100 nm (□), 200 nm (○) to 500 nm (□). Lines are Ξ calculated according to Eq. (4) for d ranging from 5 to 500 nm, from bottom to up. (b) Ξ calculated by FEM vs d for various Λ_0 ranging from 1 μm (black, ■), 500 nm (●), 200 nm (▲), 100 nm (▼), 50 nm (♦), 20 nm (○) to 10 nm (□). Lines are Ξ calculated according to Eq. (4) for Λ_0 ranging from 1 to 10 nm, from bottom to up.

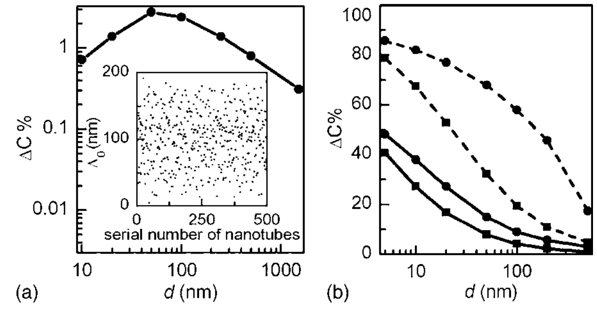

FIG. 3. (a) Relative variation of C_i (ΔC) induced by uneven Λ_0 vs d. Inset: Λ_0 associated with each nanotube in an array. (b) Relative difference between C_i of fully embedded and fully exposed nanotube arrays (ΔC) vs d. Solid lines and dashed lines represent results obtained from normal (ε_r =4.0) and high ε_r (15) dielectrics, respectively. Solid circles and squares show results obtained for Λ_0=100 nm and Λ_0=10 nm, respectively.

For the case of a SWCNT TFT device, we are interested in a solution that corresponds to the case of a uniform $\phi_i^{\text{xt}}:\phi_i^{\text{xt}}=\bar{\phi}$, $\rho_i=\bar{\rho}$. Thus, ρ is the same for each tube in the array and can be written as $\bar{\rho}=-C_Q(\bar{\phi}+\Sigma_n C_n^{-1}\bar{\rho})$, where C_n^{-1} is the reciprocal geometric capacitance between a single tube and its nth neighbor in the given array geometry. The total induced potential is $\phi_i^{\text{ind}}=\bar{\rho}\Sigma_j C_{ij}^{-1}$ and the total reciprocal capacitance of the tube is the sum of all C_n^{-1} plus C_Q^{-1}. The exact analytical expressions for C_n^{-1} and the sum $C_\infty^{-1}=\Sigma_n C_n^{-1}$ for each tube in a regular array of SWCNTs separated by the distance Λ_0 can be derived as

$$C_\infty^{-1}=\frac{1}{\varepsilon}\left(2\ln\frac{2d}{R}+2\sum_{n=1}^{\infty}\ln\frac{\Lambda_n^2+(2d)^2}{\Lambda_n^2}\right)=\left(\frac{2}{\varepsilon}\ln\frac{\Lambda_0}{R}\frac{\sinh \pi 2d/\Lambda_0}{\pi}\right),\tag{3}$$

where Λ_n is the distance between a given tube and its nth neighbor. To apply this result to the problem of SWCNT TFT, we calculate the total charge per unit area induced in the array under $\bar{\phi}$,

$$C_i=\frac{Q}{\bar{\phi}S}=\left\{\frac{2}{\varepsilon}\ln\left[\frac{\Lambda_0}{R}\frac{\sinh(\pi 2d/\Lambda_0)}{\pi}\right]+C_Q^{-1}\right\}^{-1}\Lambda_0^{-1},\tag{4}$$

where C_∞ and C_i depend on two characteristic lengths: $x=2\pi d/\Lambda_0$, which defines the intertube coupling, and $2d/R$, which defines the coupling of a single tube to the gate. The physics of the C_i coupling is clearly different for two regimes determined by x (assuming that R is always the smallest quantity). In the limit $x\ll 1$ (i.e., sparse tube density) the planar gate contribution dominates, $\sinh x\sim x$, and C_∞ reduces to that for a single, isolated tube. C_i is approximately equal to the product of the capacitance of a transistor that uses a single isolated SWCNT with the number of tubes per screening length Λ_0. In the opposite limit, $x\gg 1$, C_i approaches that of a parallel plate primarily due to the higher surface coverage of tubes. Meanwhile, C_∞ decreases due to the screening by neighboring tubes. To compare the performance of SWCNT network/array based TFTs with that of conventional TFTs that use continuous, planar channels, we calculate the ratio of the capacitance of the SWCNT array to that of a parallel plate (Fig. 2). This capacitance ratio, Ξ is close to unity for $x\gg 1$,

$$\Xi=1-\frac{\Lambda_0}{2d\pi}\frac{\varepsilon}{2}(C^{-1}+C_Q^{-1}-\log 2)+\cdots\simeq 1,\tag{5}$$

where $C^{-1}=(2\log 2d/R)/\varepsilon$ is the single tube capacitance. The term in parentheses is multiplied by the inverse tube density $1/x=\Lambda_0/2\pi d$ and is, therefore, negligible when the Λ_0 becomes much smaller than d. For $x\ll 1$, in the opposite limit, Ξ is small and grows linearly with d as given by

$$\Xi=\frac{2d\pi}{\Lambda_0}\frac{2}{\varepsilon}(C^{-1}+C_Q^{-1})^{-1}+\cdots.$$

To verify certain aspects of these calculations, we performed finite-element-method (FEM) electrostatic simulations (FEMLab, Comsol, Inc.) to determine the classical C_i of the same model system, in which the induced charge distributes itself to establish an equal potential over the nanotubes. In these calculations, R was set to 0.7 nm, which corresponds to the average radius of SWCNTs formed by chemical vapor deposition.[12] We chose ε_r=4.0. The computations, shown in Fig. 2, agree qualitatively with those determined by Eq. (4), with deviations that are most significant at small d's where quantum effects are significant.

In experimentally achievable SWCNT TFTs, the SWCNTs are not spaced equally and, except in certain cases, they are completely disordered in the form of random networks.[5,13] To estimate qualitatively the influence of uneven spacings, we constructed an array composed of five hundred parallel SWCNTs with a normal distribution of Λ_0 =100±40 nm [Fig. 3(a) inset]. C_i was calculated by inverting the matrix of potential coefficients [Eq. (1)]. The small difference of computed capacitances (ΔC) indicates that Eq. (4) can be used for aligned arrays with uneven spacings and perhaps even random SWCNT networks (Fig. 3). Another experimental fact is that most SWCNT TFTs are constructed in the bottom-gate structure where nanotubes are in an equilibrium distance above the gate dielectric, ~4 Å,[14] due to van der Waals interactions. To account for the effect of low ε air medium on C_i, we performed the FEM simulation for nanotube arrays either fully embedded in gate dielectric or fully exposed in the air. Comparing the capacitances in these two cases shows that the low ε air medium has the most significant influence on those systems that use high ε dielectrics because of the higher dielectric contrast. Moreover, at $x\ll 1$ the effect of the air on SWCNT arrays is close to the results obtained for devices based on individual tubes [Fig. 3(b)].[15] However, with increasing x, the screening between

Downloaded 12 Jan 2007 to 130.126.101.208. Redistribution subject to AIP license or copyright, see http://apl.aip.org/apl/copyright.jsp

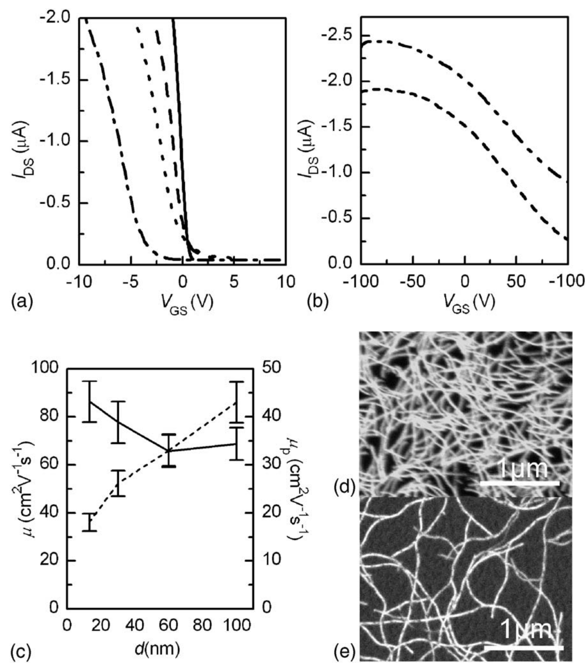

FIG. 4. (a) Drain/source current (I_{DS}) vs gate voltage (V_{GS}) at a fixed drain/source bias (V_{DS}) of −0.2 V collected from SWCNT TFTs using high density SWCNT network [SEM image shown in (d)] with a bilayer dielectric of 3 nm HfO_2 layer and an overcoat epoxy layer of 10 nm (solid line), 27.5 nm (dash line), and 55 nm (dot line) thickness or a single layer 100 nm SiO_2 (dash dot line). (b) I_{DS} vs V_{GS} collected from SWCNT TFTs using high density network (shot dash line) and low density SWCNT network [SEM image shown in part (e)] (dash dot dot line) with a single layer of 1.6 μm epoxy dielectrics. Devices have channel lengths (L) of 100 μm and effective channel widths (W) of 125 μm. (c) μ computed based on parallel plate and SWCNT array models for C_i (μ, solid line, and μ_p, dashed line, respectively).

neighboring tubes forces electric field lines to terminate on the bottom of nanotubes without fringing through the air and thus the air effect diminishes.

To explore these effects experimentally, we built TFTs that used random networks of SWCNT with fixed $1/\Lambda_0$ (approximately 10 tubes/μm, as evaluated by atomic force microscopy) and different d. Details on the device fabrication can be found elsewhere.[16] For the range of Λ_0 and d here, the difference in C_i from the air effect is less than 20%, smaller than the experimental error in determining transconductance (g_m). So Eq. (4) gives sufficiently accurate estimation of C_i. Figure 4(a) shows the transfer curves of SWCNT TFTs. Figure 4(c) compares effective mobilites calculated using C_i derived from parallel plate model to those that from Eq. (4) (μ). Consistent with the previous discussion, the parallel plate capacitor model overestimates C_i significantly for large Λ_0 or small d. As a result, the effective mobilities calculated in this manner (μ_p) have an apparent linear dependence on d that derives from inaccurate values for C_i. On the other hand, effective mobilities calculated using Eq. (4) (μ) show no systematic change with d, which provides a validation of the model.

The computed capacitances also reveal two important guidelines for the development of SWCNT TFTs. First, Eqs. (3) and (4), indicate that the effective μ should be close to the intrinsic mobility of SWCNTs ($\mu_{\text{per tube}}$) if the contact resistance is neglected since

$$\mu = \frac{L}{WC_i V_{DS}}\left|\frac{\partial I_{DS}}{\partial V_{GS}}\right| = \frac{(C_\infty^{-1}+C_Q^{-1})L}{V_{DS}}\left|\frac{\partial (I_{DS}/N)}{\partial V_{GS}}\right| \simeq \mu_{\text{per tube}}, \tag{6}$$

where N is the total number of effective pathways, connecting source/drain electrodes. μ can be smaller than $\mu_{\text{per tube}}$ because the actual length of the effective pathway is longer than L. There can also be differences between μ of devices based on SWCNT films[5,6,13] and $\mu_{\text{per tube}}$ extracted from devices based on individual tubes[17] due to influence of tube/tube junction resistances or electrostatic screening at these points that can frustrate effective gate modulation.[18] Secondly, efforts on improving g_m through increasing tube density for a given device geometry and V_{DS} are limited by d. From Fig. 2(a) we can see that at a given d, when $x \ll 1$, C_i and thus g_m increase with the increase of tube density. However, when $x \gg 1$, C_i saturates and g_m no longer increases with decreasing Λ_0. This prediction was verified by the almost identical g_m for devices with different Λ_0 on thick dielectric [Fig. 4(b)].

In summary, we evaluated C_i of SWCNT TFTs. The best electrostatic coupling between the gate and the SWCNT occurs in dense arrays of tubes, but advantage gained in C_i coupling from higher tube density starts to saturate as Λ_0 becomes close to d. These conclusions are corroborated by vertical scaling experiments on SWCNT network TFTs. We further propose two guidelines for improving the performance of SWCNT TFTs.

This work was supported by the U.S. Department of Energy under Grant No. DEFG02-91-ER45439 and the NSF through Grant No. NIRT-0403489.

[1] Q. Cao, C. Kocabas, M. A. Meitl, S. J. Kang, J. U. Park, and J. A. Rogers, in *Carbon Nanotube Electronics*, edited by A. Javey and J. Kong (Springer, Berlin, in press).
[2] C. Kocabas, M. Shim, and J. A. Rogers, J. Am. Chem. Soc. **128**, 4540 (2006).
[3] Q. Cao, S.-H. Hur, Z.-T. Zhu, Y. Sun, C. Wang, M. A. Meitl, M. Shim, and J. A. Rogers, Adv. Mater. (Weinheim, Ger.) **18**, 304 (2006).
[4] K. Bradley, J. C. P. Gabriel, and G. Grüner, Nano Lett. **3**, 1353 (2003).
[5] E. S. Snow, P. M. Campbell, M. G. Ancona, and J. P. Novak, Appl. Phys. Lett. **86**, 033105 (2005).
[6] S.-H. Hur, C. Kocabas, A. Gaur, M. Shim, O. O. Park, and J. A. Rogers, J. Appl. Phys. **98**, 114302 (2005).
[7] J. Guo, S. Goasguen, M. Lundstrom, and S. Datta, Appl. Phys. Lett. **81**, 1486 (2002).
[8] S. V. Rotkin, in *Applied Physics of Nanotubes*, edited by Ph. Avouris (Springer, Berlin, 2005), pp. 3–39.
[9] S. V. Rotkin (unpublished).
[10] K. A. Bulashevich and S. V. Rotkin, JETP Lett. **75**, 205 (2002).
[11] S. Rosenblatt, Y. Yaish, J. Park, J. Gore, V. Sazonova, and P. L. McEuen, Nano Lett. **2**, 869 (2002).
[12] Y. Li, W. Kim, Y. Zhang, M. Rolandi, D. Wang, and H. Dai, J. Phys. Chem. B **105**, 11424 (2001).
[13] C. Kocabas, S. H. Hur, A. Gaur, M. A. Meitl, M. Shim, and J. A. Rogers, Small **1**, 1110 (2005).
[14] D. Qian, G. J. Wagner, W. K. Liu, M.-F. Yu, and R. S. Ruoff, Appl. Mech. Rev. **55**, 495 (2002).
[15] O. Wunnicke, Appl. Phys. Lett. **89**, 083102 (2006).
[16] Q. Cao, M.-G. Xia, M. Shim, and J. A. Rogers, Adv. Funct. Mater. **16**, 2355 (2006).
[17] X. J. Zhou, J. Y. Park, S. M. Huang, J. Liu, and P. L. McEuen, Phys. Rev. Lett. **95**, 146805 (2005).
[18] A. A. Odintsov, Phys. Rev. Lett. **85**, 150 (2000).

Downloaded 12 Jan 2007 to 130.126.101.208. Redistribution subject to AIP license or copyright, see http://apl.aip.org/apl/copyright.jsp